

# Quantifying the impact of ecological memory on the dynamics of interacting communities

Moein Khalighi<sup>1\*†</sup>, Guilhem Sommeria-Klein<sup>1†</sup>, Didier Gonze<sup>2</sup>, Karoline Faust<sup>3</sup>, Leo Lahti<sup>1\*</sup>

**1** Department of Computing, Faculty of Technology, University of Turku, Finland

**2** Unité de Chronobiologie Théorique, Faculté des Sciences CP 231, Université Libre de Bruxelles, Belgium

**3** Laboratory of Molecular Bacteriology (Rega Institute), Department of Microbiology, Immunology and Transplantation, KU Leuven, Leuven, Belgium

\* Corresponding authors

moein.khalighi@utu.fi (MKH)

leo.lahti@utu.fi (LL)

† Equal contribution

## Abstract

Ecological memory refers to the influence of past events on the response of an ecosystem to exogenous or endogenous changes. Memory has been widely recognized as a key contributor to the dynamics of ecosystems and other complex systems, yet quantitative community models often ignore memory and its implications.

Recent modeling studies have shown how interactions between community members can lead to the emergence of resilience and multistability under environmental perturbations. We demonstrate how memory can be introduced in such models using the framework of fractional calculus. We study how the outcomes of a well-characterized interaction model are affected by gradual increases in ecological memory under varying initial conditions, perturbations, and stochasticity.

Our results highlight the implications of memory on several key aspects of community dynamics. In general, memory introduces inertia into the dynamics. This favors species coexistence under perturbation, enhances system resistance to state shifts, mitigates hysteresis, and can affect system resilience both ways depending on the time scale considered. Memory also promotes long transient dynamics, such as

long-standing oscillations and delayed regime shifts, and contributes to the emergence and persistence of alternative stable states. Our study highlights the fundamental role of memory on ecological communities, and provides quantitative tools to introduce it in ecological models and analyse its impact under varying conditions.

## Author summary

An ecosystem is said to exhibit *ecological memory* when its future states do not only depend on its current state but also on its initial state and trajectory. Memory may arise through various mechanisms as organisms adapt to their environment, modify it, and accumulate biotic and abiotic material. It may also emerge from phenotypic heterogeneity at the population level. Despite its commonness in nature, ecological memory and its potential influence on ecosystem dynamics have been so far overlooked in many applied contexts. Here, we use modeling to investigate how memory can influence the dynamics, composition, and stability landscape of ecological communities. We incorporate long-term memory effects into a multi-species model recently introduced to investigate alternative stable states in microbial communities. We assess the impact of memory on key aspects of model behavior and validate our findings using a model parameterized by empirical data from the human gut microbiota. Our approach for modeling memory and studying its implications has the potential to improve our understanding of microbial community dynamics and ultimately our ability to predict, manipulate, and experimentally design microbial ecosystems. It could also be applied more broadly in the study of systems composed of interacting components.

## 1 Introduction

2 The temporal variations observed in ecosystems arise from the interplay of complex deterministic and  
3 stochastic processes, the identification and characterization of which requires quantitative models. The  
4 empirical study of microbial communities provides an ideal source of data to inform the development  
5 of dynamical community models, since this active research area generates dense ecological time series  
6 under highly controlled experimental conditions and perturbations [1, 2]. Nevertheless, despite the recent  
7 advances in metagenomic sequencing and other high-throughput profiling technologies that are now  
8 transforming the analysis of microbial communities [3], there has been only limited success in accurately  
9 modeling and predicting the dynamics of microbial communities, even in well-controlled laboratory  
10 conditions [2, 4, 5]. This highlights the need to re-evaluate and extend the available models to better  
11 account for the various mechanisms that underlie community dynamics [2, 6–9]. One notable shortcoming  
12 of the currently popular dynamical models of microbial communities is that they ignore the role of

13 memory, that is, they are based on the assumption that the community's future behavior solely depends  
14 on its current state, perturbations, and stochasticity.

15 Ecological memory is present when the community's past states and trajectories influence its dynamics  
16 over extended periods. This is a fundamental and ubiquitous aspect of natural communities, and its  
17 influence on community dynamics has been widely recognized across ecological systems [10–12]. Memory  
18 can emerge at different time scales through a number of mechanisms, including the accumulation of abiotic  
19 and biotic material characterizing past legacies of the system, adaptations to past conditions, dormancy,  
20 or spatial structure [13–18]. Thus, developing and investigating new means to incorporate memory  
21 in dynamical models of ecological communities has the potential to yield more accurate mechanistic  
22 understanding and predictions.

23 Diverse approaches have been proposed to explore ecological memory, including time delays [11, 19, 20],  
24 historical effects [21], exogenous memory [12], and buffering of disturbances [22]. A stochastic framework  
25 was recently used to evaluate the length, patterns, and strength of memory in a series of ecological case  
26 studies [11]. However, none of these approaches describes long-term memory with a power-law decay  
27 of the influence of past states. The lag times of antibiotic-tolerant persister cells have been shown to  
28 be power-law distributed in bacterial populations [23], and this type of long-term memory is likely to  
29 be common in microbial communities whenever memory emerges from phenotypic heterogeneity [16, 24].  
30 Furthermore, the impact of memory has not been systematically addressed in contemporary studies,  
31 and specific methods have been missing for incorporating memory into standard deterministic models of  
32 microbial community dynamics.

33 Potential community assembly mechanisms have been recently investigated based on extensions of  
34 the generalized Lotka-Volterra (gLV) model, which provides a general modeling framework for species  
35 interactions [25–27]. The standard model has been extended by incorporating external perturbations [28]  
36 and sequencing noise [29], and to satisfy specific modeling constraints such as compositionality [30, 31].  
37 gLV models have also been combined with Bayesian Networks for improved longitudinal predictions [32].  
38 One goal of these modeling efforts is to understand how alternative community types reported in the  
39 human microbiome may arise, possibly in combination with external factors [33–36]. Despite the recent  
40 popularity of gLV models in microbial ecology, the impact of memory in these models has been largely  
41 ignored.

42 We address the above shortcomings by explicitly incorporating long-term memory effects into  
43 community interaction models using fractional calculus, which provides well-established tools for modeling  
44 memory [37, 38]. We incorporate memory into a gLV model with multiplicative species interactions  
45 that was recently used to reproduce the alternative stable states observed empirically in the human gut  
46 microbiota [25], and we use this extended model to analyze and demonstrate how memory can influence

47 critical aspects of community dynamics. We then validate our findings by adding memory to a gLV model  
 48 parameterized with experimental data [39]. Our work contributes to the growing body of quantitative  
 49 techniques for studying community resistance, resilience, prolonged instability, transient dynamics, and  
 50 abrupt regime shifts [40–44].

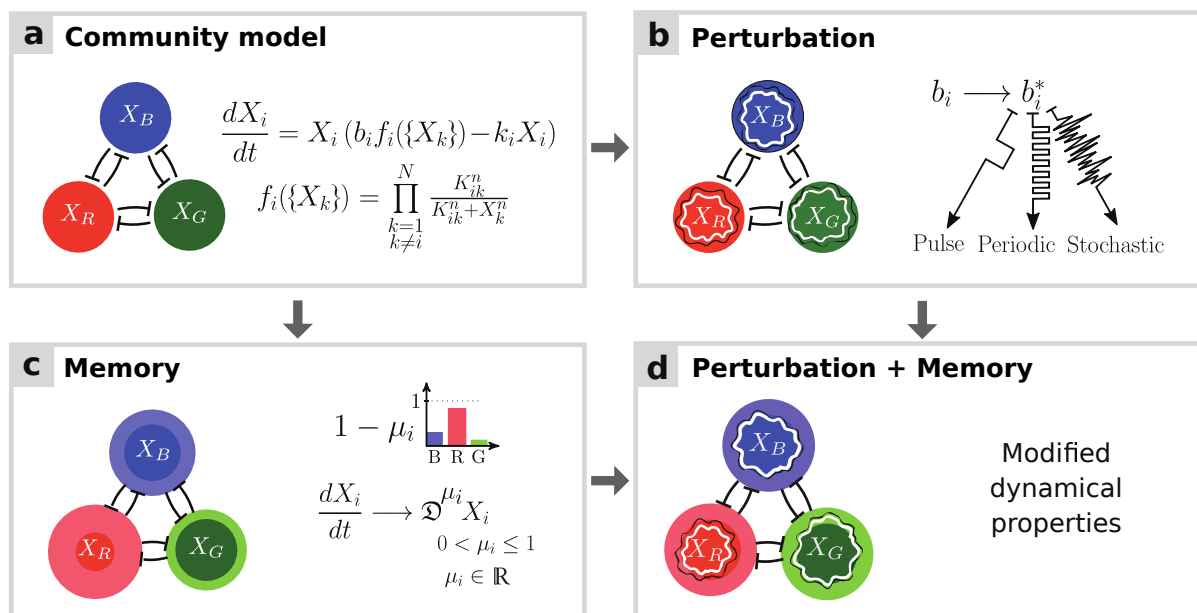


**Fig 1. Schematic illustration of a three-species community in the presence of memory and perturbations.** (a) Mutual interaction model introduced by Gonze et al. [25] to illustrate the emergence of alternative stable states in human gut microbial communities. The model describes the dynamics of species abundances  $X_i$  as functions of growth rates  $b_i$ , death rates  $k_i$ , and inhibition functions  $f_i$ , where  $K_{ij}$  and  $n$  denote interaction constants and Hill coefficients, respectively. (b) Standard perturbations include pulse, periodic, and stochastic variation in species immigration, death, or growth rates. Such perturbations may trigger shifts between alternative states. (c) Memory (bolded circles) can be incorporated into dynamical models by substituting the integer-order derivatives with fractional derivatives  $\mathfrak{D}^{\mu_i}$  of order  $\mu_i$  (see [37] and Methods). As decreasing  $\mu_i$  values correspond to increasing memory, memory is measured as  $1 - \mu_i$ . When all community members have the same memory ( $\mu_i = \mu$  for all  $i$ ), the system is said to have *commensurate* memory, otherwise *incommensurate*. Increasing memory changes community dynamics, in particular by introducing inertia and modifying the stability landscape around stable states. (d) Ecological memory can change the system dynamics under perturbations.

## 51 Results

### 52 Modeling memory

53 The gLV and its extensions are ordinary differential equation systems. This class of models has been  
 54 commonly used to model community dynamics, but their standard formulations ignore memory effects.  
 55 Here, we show how ecological memory can be included in these models using *fractional calculus*. This  
 56 mathematical tool provides a principled framework for incorporating memory effects into differential  
 57 equation systems (see *e.g.* [37, 38, 45]), thus allowing a systematic analysis and quantification of memory

58 effects in commonly used dynamical models of ecological communities.

59 Let us first consider a simple community with three species that tend to inhibit each other's growth  
60 (Fig 1a). We will later extend this model community to a larger number of species. To model this system,  
61 we employ a non-linear extension of the gLV model that was recently used to demonstrate possible  
62 mechanisms underlying the emergence of alternative states in a community [25]. This model describes  
63 the dynamics of a species  $i$  as a function of its growth rate, death rate, and a multiplicative interaction  
64 term function of the interaction matrix between all species pairs, as described in Fig 1a. Under certain  
65 conditions, this model gives rise to a tristable community, where each stable state corresponds to the  
66 dominance of a different species. The community can shift from one stable state to another following a  
67 perturbation (Fig 1b). Such transitions can be for instance controlled by changes in the species' growth  
68 rates.

69 To introduce memory, we extend this model by incorporating fractional derivatives. In this extended  
70 formulation, the classical derivative operator  $d/dt$  is replaced by the fractional derivative operator  $\mathfrak{D}^{\mu_i}$ ,  
71 where  $\mu_i \in (0, 1]$  is the non-integer derivative order for species  $i$  (Fig 1c). The fractional derivative is  
72 defined by a convolution integral with a power-law memory kernel (see Methods). The  $\mu_i$  can then be  
73 used as a tuning parameter for memory, with lower values of  $\mu_i$  indicating higher levels of memory for  
74 species  $i$  [37]. The *strength of memory* for species  $i$  is measured as  $1 - \mu_i$ . This model includes two special  
75 cases: (i) *no memory* ( $\mu_i = \mu = 1$  for all species  $i$ ), which corresponds to the original community model  
76 with classical integer-order derivatives, and (ii) *commensurate memory*, where all species have equal  
77 memory ( $\mu_i = \mu \leq 1$ ). In contrast, the general case is referred to as *incommensurate memory*, where  $\mu_i$   
78 may be unique for each  $i$ , and hence the degree of memory may differ between species. We numerically  
79 solve the fractional-order model with varying values of the parameter  $\mu_i$ , thus inducing varying levels  
80 of memory, and use it to analyse the effect of memory on various aspects of community dynamics, in  
81 particular its response to perturbations (Fig 1d).

## 82 Resistance and resilience to perturbation

83 *Resistance* refers to a system's capacity to withstand a perturbation without changing its state, while  
84 *resilience* refers to its capacity to recover to its original state after a perturbation [46, 47]. To examine  
85 the impact of ecological memory on community resistance and resilience in response to perturbations, we  
86 perturbed the system by changing the species growth rates over time. Specifically, we investigated the  
87 three-species community under *pulse* (Fig 2), *periodic* (Fig 3), and *stochastic* (Fig 4) perturbations, and  
88 analysed the impact of these three types of perturbations on community dynamics in the presence of  
89 (commensurate) memory.

90 Our results show that memory tends to increase resistance to perturbations by allowing the competing

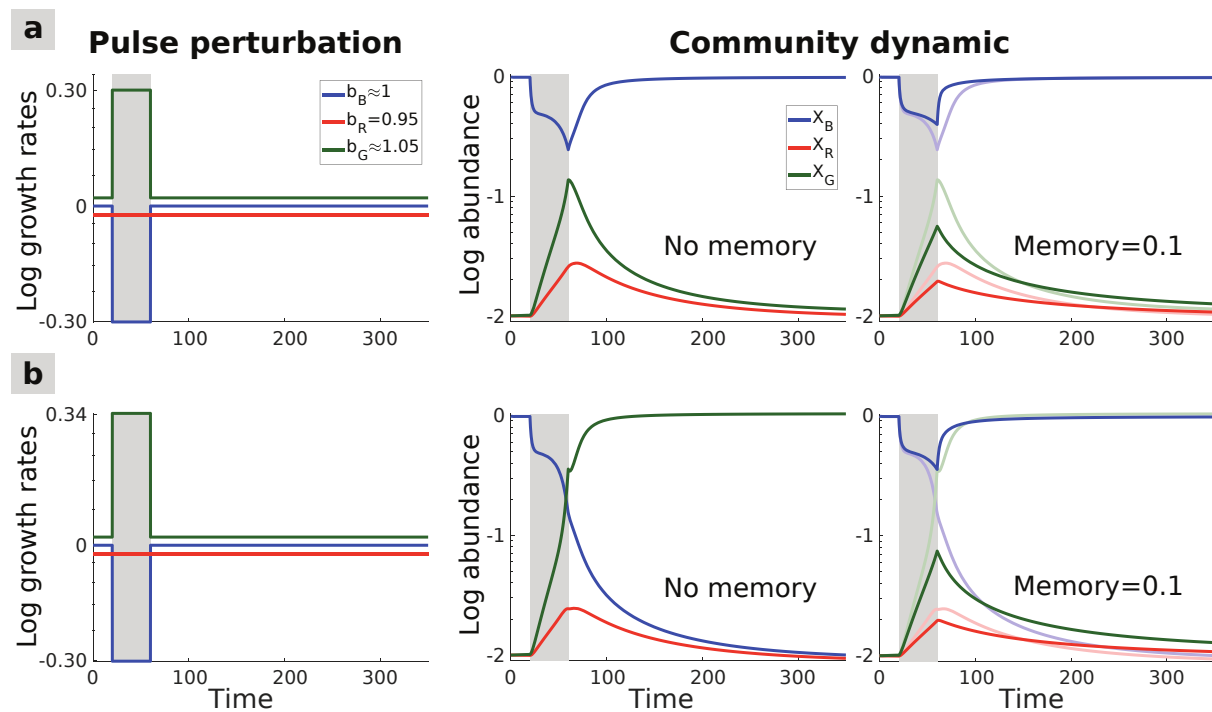


**Fig 2. Impact of commensurate memory on community resistance and resilience.** (a) A pulse perturbation is applied to the community (left panel): the growth rate of the blue species is lowered while that of the green species is simultaneously raised. The perturbation temporarily moves the community away from its initial stable state, characterized by blue species dominance (middle panel). Introducing commensurate memory (right panel) increases resistance to perturbation since the community is not displaced as far from its initial state compared to the memoryless case (shown in superimposition). The effect on resilience depends on the time scale considered: while memory initially hastens the recovery after the perturbation, it slows down the later stages of the recovery (starting around the time step 150). (b) A slightly stronger pulse perturbation is applied (left panel), triggering a shift toward an alternative stable state dominated by the green species (middle panel). Memory can prevent the state shift (right panel). Thus, here, not only does memory increase community resistance to perturbation, but also resilience as manifested by the prevented state shift.

91 species' coexistence for a longer time. In the presence of memory, switches between alternative community  
 92 states take place more slowly following a pulse perturbation (Fig 2a), or in some cases may be prevented  
 93 entirely (Fig 2b). S1 Fig provides a further example of the increased resistance provided by memory in a  
 94 larger, unstructured community where memory helps preserve the stable state after a pulse perturbation  
 95 compared to the corresponding memoryless system.

96 After the perturbation has ceased, memory initially hastens the return to the original state, but then  
 97 slows it down in the later stages of the recovery (Fig 2a). Thus, the impact of memory on resilience is  
 98 multi-faceted: depending on the time scale considered, memory either hastens or slows down the recovery  
 99 from perturbations, thus increasing or reducing resilience, respectively. Long-term memory may indeed  
 100 act across several time scales owing to the slow (here power-law) decay of the influence of past states.  
 101 Furthermore, in multistable systems, memory enhances resilience by promoting the persistence of the  
 102 original stable state (Fig 2b).

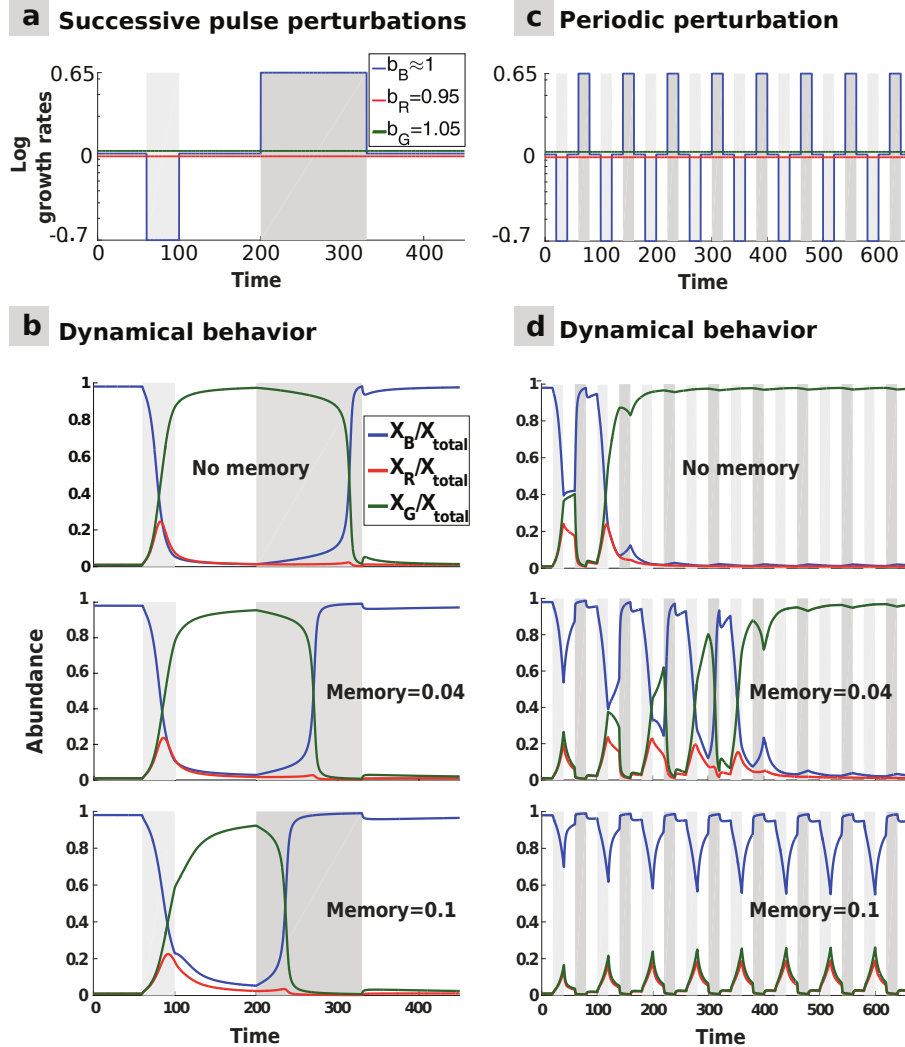


**Fig 3. Multi-pulse and periodic perturbations: commensurate memory impact on hysteresis and transient oscillations.** (a) Two opposite pulse perturbations are applied successively: the blue species growth rate is first briefly lowered, and then raised for a longer time. (b) The top panel shows the hysteresis in the system: the state shift towards the dominance of the green species occurs faster after the first perturbation than the shift back to the initial stable state after the second perturbation. Introducing commensurate memory (middle and bottom panels) delays the first state shift, thus increasing resistance, and hastens the second state shift, thus mitigating the hysteresis effect and increasing long-term resilience. (c) Rapidly alternating opposite perturbations are applied to the blue species growth rate with a regular frequency. (d) Without memory (top), the hysteresis effect leads to a permanent shift towards the green-dominated alternative stable state after a few oscillations. Adding commensurate memory mitigates the hysteresis, thus extending the transitory period (middle), which may generate longstanding oscillations in community composition before the community converges to a stable state (bottom).

103 Considering two successive pulse perturbations in opposite directions (Fig 3a) highlights another way  
104 memory can affect resilience in multistable systems. After a state shift triggered by a first perturbation,  
105 memory hastens recovery to the initial state following a second, opposite perturbation, hence increasing  
106 long-term resilience (Fig 3b). Memory can thus mitigate the hysteresis that is typical of many ecological  
107 systems.

108 In the presence of regularly alternating opposite pulse perturbations (Fig 3c), akin to those experienced  
109 by the gut microbiome or marine plankton, the community may not be able to recover its initial state if  
110 the perturbations follow each other too rapidly. In such circumstances, memoryless communities reach a  
111 new stable state faster than the communities with memory, as the latter resist the perturbations for a  
112 longer time because of the reduced hysteresis (Fig 3d). This may lead to community dynamics being  
113 trapped in long-lasting transient oscillations.

114 Finally, we analyse the role of stochastic perturbations, which form an essential component of variation  
115 in real systems. Under stochastic perturbation (Fig 4a), ecological memory dampens the fluctuations and  
116 can significantly delay the shift towards an alternative stable state (Fig 4b). This demonstrates in a more  
117 realistic perturbation setting how memory promotes community resistance to perturbation. Our results  
118 thus show that memory can enable long-term species coexistence under stochastic or alternating pulse  
119 perturbations.

120 Memory can have unexpected effects on community dynamics when its strength is tuned to bring the  
121 system in the vicinity of the tristable region, where the outcome of the dynamics is highly sensitive to  
122 initial conditions. Under such conditions, minute changes in memory can push the system over a tipping  
123 point towards another attractor, radically changing the outcome (Fig 4c). This illustrates that, beyond  
124 introducing inertia into the dynamics and damping perturbations, memory can have non-trivial effects on  
125 the system's stability landscape, which we investigate in the next section.

## 126 Impact on stability landscape

127 Let us now consider a tristable model equivalent to the one used so far, where the 3-species community  
128 is replaced for more generality by a 15-species community structured into three groups through its  
129 interaction matrix. Each of these groups represents a set of weakly competing species—*e.g.*, because  
130 of cross-feeding interactions that mitigate competition, whereas species belonging to different groups  
131 compete more strongly with each other (Fig 5a). We show that adding memory in such a system can  
132 change the outcome of the dynamics even in the absence of perturbation. In particular, increasing the  
133 strength of (incommensurate) memory in the group that is dominant in the stable state of the memoryless  
134 system can lead to its exclusion from the new stable state (Fig 5b-c). This happens because memory  
135 shifts the boundary between stable states in the space of initial conditions.

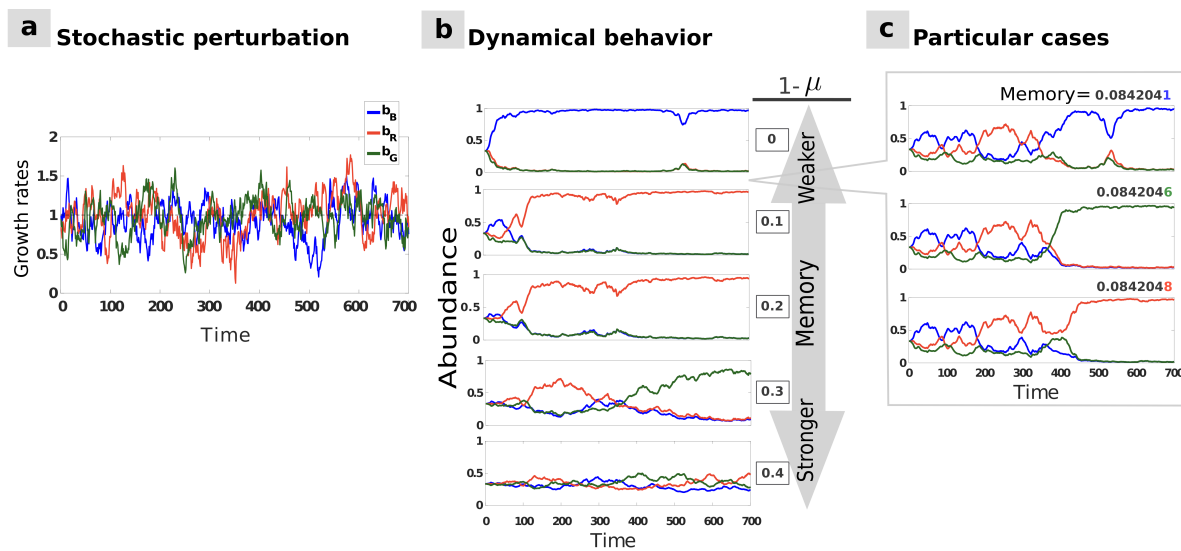


**Fig 4. Stochastic perturbations with commensurate memory effects.** (a) Species growth rates  $b_i$  vary stochastically through time according to an Ornstein-Uhlenbeck process (see Table in S1 Table). (b) Dynamical behavior of the system in response to the stochastic perturbation for equal initial species abundances and varying memory level: in addition to slowing down community dynamics, increasing memory limits the overall variation in species abundances, thus enhancing the overall resistance of the system and promoting species coexistence. (c) For some memory strengths, the final state of the system can be sensitive to slight variations in memory, with drastic consequences on community composition.

136 Adding memory in a given species may lead to either a reduction or an increase in its abundance  
 137 depending on the conditions. Whereas Fig 5b-c and S2 Fig illustrate the exclusion of a group of species  
 138 with higher memory from the stable state in the absence of perturbation, memory may conversely increase  
 139 the persistence or abundance of a species, as illustrated in S3b Fig in the presence of perturbation. In  
 140 fact, in the presence of perturbation, tuning memory in a given species may lead to the dominance of any  
 141 of the species depending on the perturbation and initial conditions. This result holds both in the case of  
 142 pulse (S3a Fig) and stochastic (S3b Fig) perturbation.

143 When setting the memory strength close to the threshold value between two alternative stable states  
 144 for a given initial condition, we observe long transient dynamics where the community may remain stuck  
 145 in an unstable state for an extended period of time. After a long period of subtle, gradual changes, the  
 146 community eventually converges to its stable state in an abrupt regime shift that is not triggered by any  
 147 perturbation or changes in the model parameters (Fig 5d).

148 Remarkably, memory can also induce similar long transient dynamics when the system is outside the  
 149 region of the model's parameter space exhibiting multistability. S4 Fig illustrates how, depending on  
 150 initial conditions, incommensurate memory may induce long transient states in a community that would,  
 151 in the absence of memory, rapidly converge to a single stable state irrespective of initial conditions. These  
 152 transient states are characterized by the dominance of a species or group of species that is not dominant  
 153 in the stable state. A bifurcation diagram shows that the region of the model's parameter space that

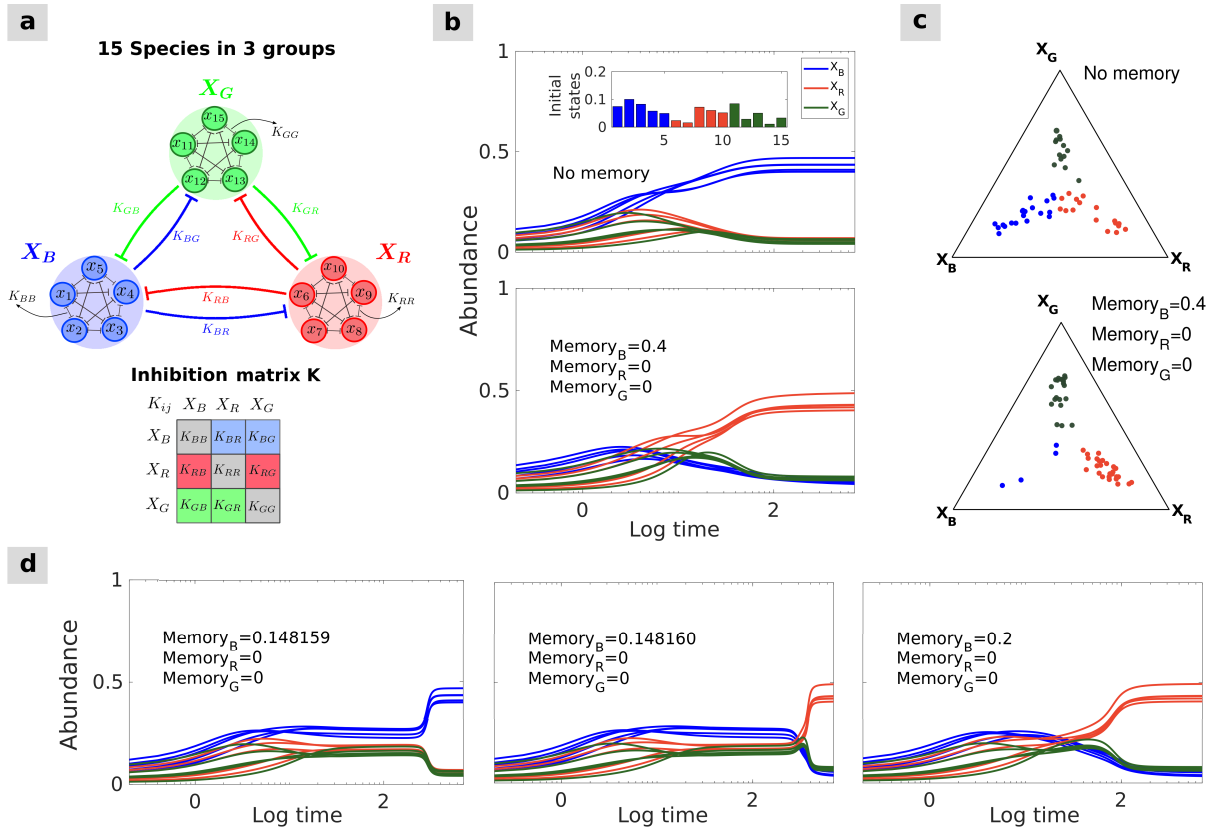


**Fig 5. Impact of incommensurate memory on the community stability landscape: regime shifts without perturbation.** (a) A 15-species version of Gonze's mutual interaction model (see Gonze et al. [25]). The 15 species form three groups, blue, red, and green, and within-group species interactions are stronger than between-group interactions. The resulting system exhibits three stable states, each dominated by a different group. (b) Starting from random initial conditions, the blue group of species dominates the community in the stable state when no memory is present (top). Starting from the same initial conditions, imposing memory on the blue species leads to a temporary rise in abundance, but ultimately another (red) group of species dominates instead (bottom). (c) Ternary plots represent the stable state distributions of 50 simulations with random initial conditions and noise in model parameters. Each dot shows, for one simulation at convergence time, the identity of the dominant group (color) and the average relative abundances of the three groups (position in the triangle; see S1 Appendix for details). In the memoryless system (top), the three groups roughly have the same chance of dominating the stable state, whereas imposing memory effects on the blue set of species (bottom) favors stable states where those species are not dominant. (d) Setting incommensurate memory in the blue species around the threshold separating two stable states (here, 0.14816) leads to an abrupt regime shift after a long period of subtle, gradual inclines, without changing any model parameters or adding noise.

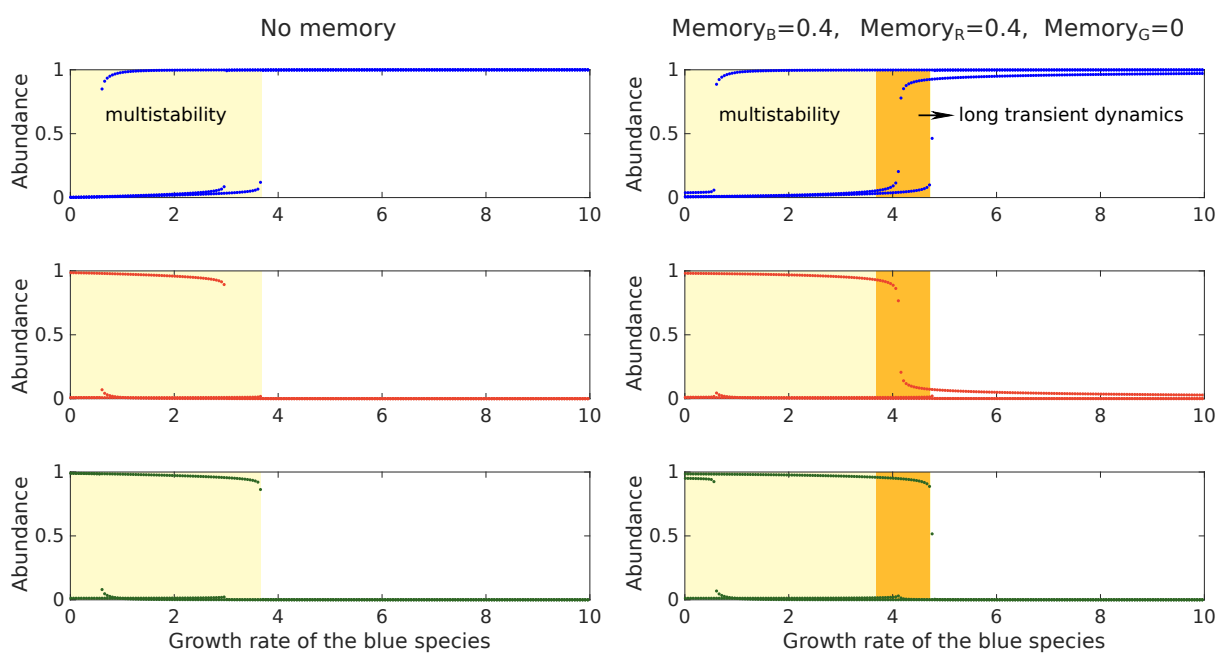


**Fig 6. Memory induces long transient dynamics in a region of the parameter space adjacent to the multistable region.** Bifurcation diagrams for the 3-species Gonze model showing the relative abundances at time 1,000 of the blue, red, and green species as functions of the blue species' growth rate, for three different initial conditions (leading to three distinct curves per plot), and in the absence (left column) or presence (right column) of memory. The light and dark yellow regions exhibit several alternative states for the same parameter values. However, it can be shown analytically that the system only admits a single stable state in the dark yellow region, whereas it admits multiple stable states in the light yellow region. Therefore, alternative states at time 1,000 in the dark yellow region correspond to instances of long transient dynamics, where the system remains stuck near ghost attractor states. See S4 Fig for illustrations of the dynamics in the dark yellow region.

154 exhibits long transient dynamics is next to the multistability region (Fig 6). Memory therefore reveals  
 155 the “imprint” of alternative stable states that exist in adjacent regions of the parameter space.

## 156 Empirically parameterized model

157 Our approach to modeling memory effects is general and could be applied to any differential equation  
 158 system. To validate some of our results in a more realistic setting, we applied our approach to a gLV  
 159 system that has been parameterized with extensive experimental data from synthetic human gut microbial  
 160 communities [39]. For demonstration purposes, we restricted ourselves to communities of just two  
 161 species, which we formed by virtually combining the following bacterial species: *Bacteroides uniformis*  
 162 (BU), *Bacteroides thetaiotaomicron* (BT), *Clostridium hiranonis* (CH), and *Eubacterium rectale* (ER).  
 163 We analyzed three different combinations of two species: (i) combining BU and BT, we obtained a  
 164 *bistable* community converging to distinct stable states depending on initial conditions, similarly to the  
 165 communities investigated so far (S5c-d Fig); (ii) combining CH and ER, we obtained a monostable  
 166 community exhibiting *stable coexistence*, where neither of the species makes up more than 95% of the  
 167 total abundance in the stable state (S5e Fig); and (iii) combining BT and CH, we obtained a monostable

168 community exhibiting *single species dominance* in the stable state (S5f Fig). We compared the results  
169 obtained by introducing memory in these empirically parameterized communities with those obtained  
170 in a two-species version of the multistable (here bistable) model studied so far, hereafter referred to as  
171 Gonze model. We systematically tested a wide range of memory strength values to assess the robustness  
172 of our results.

173 We first measured the resistance and resilience of the two bistable community types (i.e., the BU-BT  
174 community and the two-species Gonze model) to a pulse perturbation. We measured resistance as  
175 the strongest perturbation the community can withstand before shifting to an alternative stable state  
176 (see Resistance and resilience metrics). In agreement with our previous results, we find that memory  
177 consistently increases resistance over the tested range of memory strengths (S6 Fig and S7 Fig). We  
178 measured resilience as the recovery time to the stable state after perturbation. In agreement with our  
179 previous results, we find that memory hastens the recovery over short time scales and (S8a Fig and  
180 S9a Fig) but slows it down over longer time scales (S8b Fig and S9b Fig).

181 We then measured the convergence time to the stable state in the absence of perturbation under varying  
182 memory strength in all community types, that is, in the three empirically parameterized communities  
183 as well as in the two-species Gonze model. In all cases, introducing memory lengthens the convergence  
184 time to the stable state, illustrating the inertia induced by memory (S10-S13 Fig). Nevertheless, in the  
185 two bistable communities, introducing memory reduces the convergence time in cases where memory  
186 leads to a change in stable state (S10 Fig and S11 Fig). Interestingly, in every community type, varying  
187 the level of memory in the two species independently (i.e., introducing incommensurate memory) shows  
188 that the convergence time is mostly determined by the strength of memory in the species that is less  
189 abundant in the stable state, while memory in the species that is more abundant in the stable state plays  
190 comparatively little role. This suggests that memory does not have the same influence on all species in a  
191 community, and in particular that community dynamics is more sensitive to the introduction of memory  
192 in less abundant species.

## 193 Discussion

194 Our understanding of ecological community dynamics heavily relies on mathematical modeling. Dynamical  
195 community modeling is a particularly active research area in microbial ecology, where recent studies have  
196 proposed numerous mechanistic models of microbial community dynamics exploring the role of interactions,  
197 stochasticity, and external factors [2, 25, 48–50]. These studies have, however, largely neglected the role of  
198 ecological memory despite its potentially remarkable impact on community variation. We have shown  
199 here how ecological memory can be incorporated into models of microbial community dynamics and

200 used this modeling tool to demonstrate the role of memory as a potential key determinant of community  
201 dynamics. This has allowed us to expand our understanding of the impact of memory on community  
202 response to perturbation, the emergence of alternative community states, long transient dynamics and  
203 delayed regime shifts.

204 Ecological memory is a systemic property that can arise through various mechanisms. First,  
205 memory-like delay effects may arise through intracellular mechanisms, such as cell lag phases or inertia in  
206 transcriptional regulation, which may be effectively memoryless. In such cases, the dampening effect on  
207 the dynamics may be simply modeled by introducing a break, which creates a lag in community dynamics  
208 without inducing long-term memory effects. In contrast, long-term memory may arise if communities  
209 can alter their environment and thus modify environmental parameters in ways that reflect past events,  
210 or if organisms exhibit context-specific growth rates that reflect past adaptations [51, 52]. It may also  
211 emerge only at the population or community level through phenotypic heterogeneity [23, 24], which can  
212 be favored by dormancy, spatial structure, or adaptive bet-hedging mechanisms [15–18].

213 Ecological communities are constantly subject to perturbations arising from external factors, and our  
214 analysis therefore focuses on the combined effect of perturbations and memory on community dynamics.  
215 Environmental fluctuations through time have a fundamental influence on ecological communities: they  
216 may promote species coexistence, increase community diversity [53, 54], contribute to the properties  
217 of stable states [43], and in some cases trigger abrupt regime shifts [55]. Our analysis of memory in  
218 perturbed communities is particularly relevant to recent studies analysing the response of experimental  
219 microbial communities to antibiotic pulse perturbation [1], or the impact of periodic perturbations on the  
220 evolution of antimicrobial resistance [40].

221 The emergence of alternative community states has been recently debated in the microbiome research  
222 literature [36, 56]. Gonze et al. [25] demonstrated how pulse perturbations can bring a tristable system  
223 to a boundary of the tristability region, which then triggers a transition to an alternative stable state.  
224 We have shown how introducing memory into this model can exert additional influence on the resulting  
225 dynamics and alter the community's stability landscape. We have then assessed the generality and  
226 robustness of some of our results by reproducing them in empirically parameterized models.

227 We based our modeling of memory on fractional calculus [37], an extensively studied mathematical  
228 framework that benefits from well-established mathematical properties (e.g., regarding the existence and  
229 uniqueness of solutions). It has a broad range of applications and has already been used to model memory  
230 in other fields [57, 58]. In this framework, memory is represented by fractional derivatives and their  
231 associated kernel, which determines how quickly the influence of past states fades out (see Methods, Fig 7).  
232 Fractional calculus allows introducing memory characterized by a power-law kernel, that is, a power-law  
233 decay of the influence of past states on the present state. It can be considered as a general approach to

234 the modeling of gradually declining long-term memory, such as the one emerging from phenotypically  
235 heterogeneous bacterial populations [15, 16, 23]. Hence, our qualitative results on the influence of long-term  
236 memory on community dynamics are likely to hold more generally. One major advantage of fractional  
237 calculus is that it can be readily used to introduce memory in any existing dynamical model based on  
238 ordinary or partial differential equations. It also allows for fast numerical simulations (see S2 Appendix  
239 for details). This makes the resulting models potentially suitable for simulation-based inference from  
240 data, which represents an interesting avenue for future research.

241 In general, memory adds a certain inertia in community dynamics that tends to damp down fluctuations  
242 and can therefore mitigate or prevent more extreme and sudden changes in the system. This may favor  
243 species coexistence in the presence of perturbation, and lead to qualitative changes in the dynamics and in  
244 community composition under certain conditions. We have clarified in particular how memory influences  
245 resistance and resilience to perturbations in ecological communities. An interesting line of research for  
246 future work would be to further quantify the influence of memory on the response to perturbation using  
247 recently proposed general measures of resilience, such as exit time [59]. Our findings are in agreement  
248 with previous studies showing that commensurate fractional derivatives cause intrinsic damping in a  
249 system [60, 61], which may delay transitions or shift critical thresholds [38]. Models with incommensurate  
250 memory, i.e., with different memory strengths in different species, yield differential equation systems that  
251 are mathematically more challenging to analyse, and therefore remain less well understood. Our analyses  
252 with incommensurate memory show that memory in a less abundant species tends to have a stronger  
253 influence on the overall dynamics than in a dominant one (true in most tested configurations), and that  
254 memory in a given species may or may not favor it depending on the context, such as the presence of  
255 perturbations.

256 We have shown in particular that memory can induce prolonged periods of instability [42], or long  
257 transient dynamics [44]. More specifically, memory appears to favor long “saddle point crawl-by” in  
258 regions of the parameter space that exhibit multistability, and to reinforce “ghost attractor states” in  
259 neighboring regions of the parameter space [44]. The long transient states we observed could easily be  
260 mistaken for genuine stable states over insufficiently long observation times. Long transient dynamics  
261 have previously been reported in ecological systems [62] and chemostat experiments [63], and have been  
262 linked to stochasticity, multiple time scales, and high dimensionality [44]. Ecological memory provides an  
263 alternative, and largely overlooked, mechanism for their emergence. It has been argued that regime shifts  
264 may abruptly occur without parameter changes during such long transient dynamics [44], and our results  
265 support this view since we have shown that the presence of memory can lead to abrupt regime shifts even  
266 in the absence of perturbations.

267 Several extensions of our model could be considered in future studies to enhance its flexibility and

268 to model memory more generally, such as switching memory on and off along time [38] or applying  
269 fractional differential equations with time-varying derivative orders [64]. Alternative approaches have  
270 been considered to model ecological memory: a simple approach is to incorporate autocorrelation into  
271 the model structure [20], but one could also model memory using distributed delay differential equations  
272 (DDE) [65], fractional delay differential equations [66], or memory-dependent integer derivatives [67], which  
273 allow for greater flexibility in the shape of kernel functions. However, constructing fractional derivatives  
274 analogs of standard models by using kernels other than power-law is mathematically challenging [68], and  
275 may fail to meaningfully describe long-term memory effects [69].

276 The modeling of real systems using models that incorporate memory would benefit from the ability to  
277 gather empirical evidence for the presence, strength, and type of memory in the system. Recent literature  
278 suggests that it might be possible to empirically detect the presence of memory based on the broad  
279 properties of a time series. It has been shown that longitudinal time series of microbial communities  
280 may carry detectable signatures of underlying ecological processes [7, 70]. Recently, Bayesian hierarchical  
281 models [11, 19], random forests [12], neural networks [71], and unsupervised Hebbian learning [24] have  
282 been proposed to detect signatures of memory in other contexts. Furthermore, specifically designed  
283 longitudinal experiments could be used to characterize memory in real communities. Although direct  
284 experimental manipulation of memory in a microbial system is challenging, the manipulation of lag times  
285 in *E. coli*'s diauxic shift provides a recent example [72]. We have here incorporated memory and evaluated  
286 its impact in a two-species system with experimentally obtained parameters [39], and this approach could  
287 be used to provide experimentally testable predictions on community dynamics.

288 Improving our understanding of the key mechanisms underlying community dynamics is a necessity  
289 to generate more accurate predictions, and ultimately to develop new techniques for the manipulation of  
290 ecological communities. We have combined here theoretical analysis and simulations to explore the various  
291 facets of ecological memory and highlight its often overlooked role as a key determinant of community  
292 dynamics.

## 293 Methods

294 In the following, we detail the mathematical aspects of incorporating ecological memory into two non-linear  
295 models belonging to the gLV family.

296 **Model 1: Gonze model**

297 We used, as a starting point, the following memoryless model introduced by Gonze et al. [25] and referred  
298 to in this paper as “Gonze model”:

$$\frac{dX_i}{dt} = X_i (b_i f_i(\{X_k\}) - k_i X_i),$$
$$f_i(\{X_k\}) = \prod_{\substack{k=1 \\ k \neq i}}^N \frac{K_{ik}^n}{K_{ik}^n + X_k^n}. \quad (1)$$

299 This model describes the dynamics of each microbial species abundance  $X_i$  according to its growth rate  
300  $b_i$ , its death rate  $k_i$ , and an inhibition term  $f_i$  defined by the inter-specific interaction constants  $K_{ij}$  and  
301 their exponent  $n$  (known as the Hill coefficient).  $K_{ij}$  represents the inhibition of species  $i$  by species  $j$ : the  
302 lower it is, the stronger the inhibition. Although  $X_i$  denotes absolute abundances, we represent relative  
303 abundances in most figures to ease visual comparison (except in Figs 2 and 5b,d, and in Supplementary  
304 Figures S6-S13 Fig).

305 **Three-group model.** We define three sets of species indexed by B (blue), R (red), and G (green).  
306 Each species  $i$  belongs to exactly one of these three groups. We define the growth rate of each group by  
307 the growth vector  $\mathbf{b} = [b_B, b_R, b_G]$ , where  $b_B = \{b_i \mid i \in B\}$ ,  $b_R = \{b_i \mid i \in R\}$ , and  $b_G = \{b_i \mid i \in G\}$ .  
308 We also define the inter-specific interaction matrix  $\mathbf{K} = \{K_{ij} \mid i, j \in B \text{ or } R \text{ or } G\}$  such that  $K_{ij}$  only  
309 depends on the group memberships of species  $i$  and  $j$ , plus a small noise term (see Fig 5a and Methods).  
310 We first considered a community of three species (*i.e.*, only one species per group), and then a community  
311 of 15 species forming three groups with strong inter-group inhibition and weak intra-group inhibition. If  
312 the inhibition strength is large enough (small  $K_{ij}$ ), this model can have three coexisting stable states  
313 (tristability). This tristable community is dominated by one of the three groups depending on initial  
314 species abundances, interaction matrix  $\mathbf{K}$ , and growth vector  $\mathbf{b}$ .

315 **Two-species version.** In the “Empirically parameterized model” section of the Results, we  
316 additionally use a two-species version of this model for the sake of comparison with the empirically  
317 parameterized two-species gLV models we introduce in that section (see below). This two-species version  
318 exhibits similar properties but is bistable instead of tristable, each stable state being dominated by one of  
319 species.

320 **Model 2: empirically parameterized gLV model**

321 To validate the observed impact of memory on model (1), we examined memory effects in the following  
322 dynamic species abundance model of the human gut microbiome, parameterized using in vitro interaction

323 experiments [39]:

$$\frac{dX_i}{dt} = X_i \left( b_i + \sum_{j=1}^N K_{ij} X_j \right), \quad (2)$$

324 where  $N$ ,  $b_i$ , and  $K_{ij}$  indicate the number of species, growth rates, intra-specific interaction coefficients  
325 ( $i = j$ ), and inter-specific interaction coefficients ( $i \neq j$ ), respectively. We considered four microbial  
326 species: *Bacteroides uniformis* (BU), which is negatively associated with immunological dysfunction [73],  
327 *Bacteroides thetaiotaomicron* (BT), which is positively associated with Ulcerative Colitis [74], *Clostridium*  
328 *hiranonis* (CH), and *Eubacterium rectale* (ER), which is positively associated with Type II diabetes [75].  
329 We focused on three two-species communities exhibiting different qualitative behaviors: coexistence (CH  
330 and ER, with +/- interaction), dominance (BT and CH, with -/- interaction), and bistability (BU and  
331 BT, with -/- interaction). The interaction coefficients and growth rates are based on the training set T3  
332 from Venturelli et al. [39].

### 333 Incorporating memory using fractional calculus

334 Fractional order derivatives have been successfully used to account for memory effects in many disciplines [37,  
335 38,57]. To introduce memory in the initial models defined by equations (1) and (2), we replaced the ordinary  
336 first-order time derivatives by fractional derivatives  $\mathfrak{D}^{\mu_i}$  (more precisely, Caputo fractional derivatives [76]).  
337 These modified models can be expressed, using the simplifying notation  $F_i := X_i (b_i f_i(\{X_k\}) - k_i X_i)$  or  
338  $F_i := X_i \left( b_i + \sum_{j=1}^N K_{ij} X_j \right)$ , as:

$$\mathfrak{D}^{\mu_i} X_i = F_i, \quad 0 < \mu_i \leq 1, \mu_i \in \mathbb{R}. \quad (3)$$

339 Fractional derivatives implicitly introduce a time correlation function, or “memory kernel”, which  
340 imposes a dependency between the current system state and its past trajectory via a convolution integral  
341 (Fig 7a). That is to say, equation (3) can also be expressed using a first-order derivative, as:

$$\frac{dX_i(t)}{dt} = \int_{t_0}^t K_{\mu_i}(t - \tau) F_i(\tau) d\tau. \quad (4)$$

342 The memory kernel’s decay rate depends on  $\mu_i$ : the lower the value of  $\mu_i$ , the slower it will decay (Fig 7).  
343 Throughout this article, we quantify memory as  $1 - \mu_i$ . In the memoryless case ( $\mu_i = 1$ ), the kernel  
344 becomes a Dirac delta function,  $\delta(t - \tau)$ , which results in an ordinary integer-order differential equation.  
345 For  $0 < \mu_i < 1$ , the memory thus introduced can be considered to have a power-law decay in time, a  
346 temporal scaling behavior that is common in nature [23,58,61,62,77]. Indeed, it can be shown that there  
347 is a parameter  $\mu > 0$  such that the limit  $\lim_{t \rightarrow \infty} t^{-\mu} K_\mu(t - \tau)$  is a finite constant for fixed  $\tau$  [78]. Efficient  
348 numerical methods exist to solve fractional-order differential equation systems (see S2 Appendix).

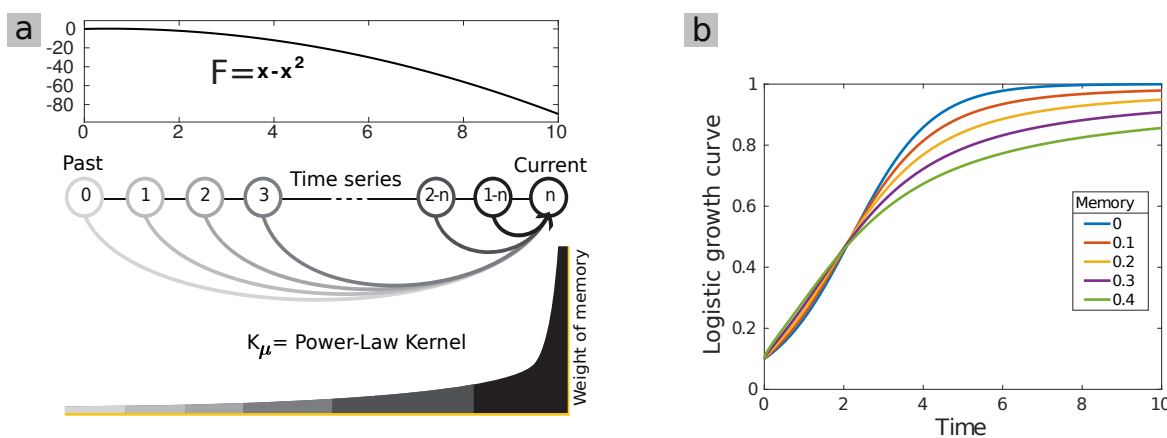


**Fig 7. An intuitive interpretation of the memory introduced by fractional derivatives and of its effect on convergence time for the logistic curve. (a)** The  $F$  function in equation (4) for the standard logistic equation, and a sketch of the memory effects introduced by fractional derivatives on a time series: the weight of past states on the present decreases as a power-law of time. **(b)** Influence of a range of memory strengths on the classic logistic growth curve.

### 349 Resistance and resilience metrics

350 We define here quantitative metrics of resistance and resilience, which we use to rigorously investigate and  
 351 summarise the influence of memory on the two-species community models analyzed in the “Empirically  
 352 parameterized model” section of the results.

353 **Convergence time:** To measure the time of convergence to the stable state, we measured through  
 354 time the Bray-Curtis dissimilarity between the current state of the community, defined by the set  
 355 of the abundances of all its component species, and its stable state, corresponding to a fixed point  
 356 of the dynamical system. We measured Bray-Curtis dissimilarity between communities 1 and 2 as  
 357  $BC = \left( \sum_{i=1}^S |X_{i,1} - X_{i,2}| \right) / \left( \sum_{i=1}^S (X_{i,1} + X_{i,2}) \right)$ , where  $X_{i,1}$  and  $X_{i,2}$  are the absolute abundances of  
 358 species  $i$  in community 1 and 2 and  $S$  is the total number of species. We considered the community to have  
 359 converged once this dissimilarity was lower than a certain threshold, referred to as the convergence interval.  
 360 In some cases, we then compared the convergence times obtained with more or less stringent convergence  
 361 intervals. We used this approach to quantify the convergence time to stability in Supplementary Figures  
 362 S8-S13 Fig.

363 **Resistance:** We measured resistance to perturbation of a multistable community as the strongest  
 364 perturbation for which the community still recovers to its initial stable state (instead of shifting to an  
 365 alternative stable state). We used this approach in S6 Fig and S7 Fig to quantify the resistance of  
 366 two-species bistable communities to a pulse perturbation in the growth rate of one of the species, starting  
 367 from the stable state. The intensity of the perturbation is defined as the value at which the growth rate  
 368 is set during the pulse.

369 **Resilience:** We measured resilience to perturbation as the recovery time to the initial stable state

370 after a perturbation. We used the strongest perturbation for which the community still recovers to its  
371 initial stable state. We measured the recovery time as the convergence time to the stable state. We used  
372 this approach in S8 Fig and S9 Fig to quantify the resilience of two-species bistable communities to a  
373 pulse perturbation, as above.

374 **Data availability**

375 The computational results for this article have been generated with MATLAB. All data and code used  
376 for running the simulations and generating the figures is available in GitHub, and accessible via the  
377 permanent Zenodo DOI: <https://doi.org/10.5281/zenodo.5979561>.

378 **References**

- 379 1. Cairns J, Jokela R, Becks L, Mustonen V, Hiltunen T. Repeatable ecological dynamics govern  
380 the response of experimental communities to antibiotic pulse perturbation. *Nat Ecol Evol.*  
381 2020;4(10):1385–1394. doi:10.1038/s41559-020-1272-9.
- 382 2. Gonze D, Coyte KZ, Lahti L, Faust K. Microbial communities as dynamical systems. *Curr Opin*  
383 *Microbiol.* 2018;44:41–49. doi:10.1016/j.mib.2018.07.004.
- 384 3. Quince C, Walker AW, Simpson JT, Loman NJ, Segata N. Shotgun metagenomics, from sampling  
385 to analysis. *Nat biotechnol.* 2017;35(9):833–844. doi:10.1038/nbt.3935.
- 386 4. Widder S, Allen RJ, Pfeiffer T, Curtis TP, Wiuf C, Sloan WT, et al. Challenges in microbial  
387 ecology: building predictive understanding of community function and dynamics. *The ISME*  
388 *Journal.* 2016;10(11):2557–2568. doi:10.1038/ismej.2016.45.
- 389 5. Bosi E, Bacci G, Mengoni A, Fondi M. Perspectives and Challenges in Microbial Communities  
390 Metabolic Modeling. *Front genet.* 2017;8. doi:10.3389/fgene.2017.00088.
- 391 6. Song HS, Cannon WR, Beliaev AS, Konopka A. Mathematical Modeling of Microbial Community  
392 Dynamics: A Methodological Review. *Processes.* 2014;2(4):711–752. doi:10.3390/pr2040711.
- 393 7. Faust K, Bauchinger F, Laroche B, De Buyl S, Lahti L, Washburne AD, et al. Signatures  
394 of ecological processes in microbial community time series. *Microbiome.* 2018;6(1):1–13.  
395 doi:10.1186/s40168-018-0496-2.
- 396 8. Coenen AR, Hu SK, Luo E, Muratore D, Weitz JS. A Primer for Microbiome Time-Series Analysis.  
397 *Front genet.* 2020;11:310–310. doi:10.3389/fgene.2020.00310.

398 9. Björk JR, Dasari M, Grieneisen L, Archie EA. Primate microbiomes over time: Longitudinal  
399 answers to standing questions in microbiome research. *Am J Primatol.* 2019;81(10-11):e22970.  
400 doi:10.1002/ajp.22970.

401 10. Johnstone JF, Allen CD, Franklin JF, Frelich LE, Harvey BJ, Higuera PE, et al.  
402 Changing disturbance regimes, ecological memory, and forest resilience. *Front Ecol Environ.*  
403 2016;14(7):369–378. doi:10.1002/fee.1311.

404 11. Ogle K, Barber JJ, Barron-Gafford GA, Bentley LP, Young JM, Huxman TE, et al.  
405 Quantifying ecological memory in plant and ecosystem processes. *Ecol Lett.* 2015;18(3):221–235.  
406 doi:10.1111/ele.12399.

407 12. Benito BM, Gil-Romera G, Birks HJB. Ecological memory at millennial time-scales: the  
408 importance of data constraints, species longevity and niche features. *Ecography.* 2020;43(1):1–10.  
409 doi:10.1111/ecog.04772.

410 13. Schweiger AH, Boulangeat I, Conradi T, Davis M, Svenning JC. The importance of ecological  
411 memory for trophic rewilding as an ecosystem restoration approach. *Biol Rev.* 2019;94(1):1–15.  
412 doi:10.1111/brv.12432.

413 14. Žliobaitė I, Fortelius M, Stenseth NC. Reconciling taxon senescence with the Red Queen’s hypothesis.  
414 *Nature.* 2017;552(7683):92–95. doi:10.1038/nature24656.

415 15. Skanata A, Kussell E. Ecological memory preserves phage resistance mechanisms in bacteria. *Nat  
416 Commun.* 2021;12(1):6817. doi:10.1038/s41467-021-26609-w.

417 16. Gokhale CS, Giaimo S, Remigi P. Memory shapes microbial populations. *PLoS Comput Biol.*  
418 2021;17(10):1–16. doi:10.1371/journal.pcbi.1009431.

419 17. Miyaue S, Suzuki E, Komiyama Y, Kondo Y, Morikawa M, Maeda S. Bacterial memory of  
420 persisters: bacterial persister cells can retain their phenotype for days or weeks after withdrawal  
421 from colony–biofilm culture. *Front microbiol.* 2018;9. doi:10.3389/fmicb.2018.01396.

422 18. Mutlu A, Trauth S, Ziesack M, Nagler K, Bergeest JP, Rohr K, et al. Phenotypic memory in  
423 *Bacillus subtilis* links dormancy entry and exit by a spore quantity-quality tradeoff. *Nat Commun.*  
424 2018;9(1):69. doi:10.1038/s41467-017-02477-1.

425 19. Itter MS, Vanhatalo J, Finley AO. EcoMem: An R package for quantifying ecological memory.  
426 *Environ Model Softw.* 2019;119:305–308. doi:10.1016/j.envsoft.2019.06.004.

427 20. Golinski M, Bauch C, Anand M. The effects of endogenous ecological memory on  
428 population stability and resilience in a variable environment. *Ecol Model.* 2008;212(3):334–341.  
429 doi:10.1016/j.ecolmodel.2007.11.005.

430 21. Schaefer V. Alien invasions, ecological restoration in cities and the loss of ecological memory. *Restor  
431 Ecol.* 2009;17(2):171–176. doi:10.1111/j.1526-100X.2008.00513.x.

432 22. Bengtsson J, Angelstam P, Elmquist T, Emanuelsson U, Folke C, Ihse M, et al. Reserves, resilience  
433 and dynamic landscapes. *Ambio.* 2003;32(6):389–396. doi:10.1579/0044-7447-32.6.389.

434 23. Şimşek E, Kim M. Power-law tail in lag time distribution underlies bacterial persistence. *PNAS.*  
435 2019;116(36):17635–17640. doi:10.1073/pnas.1903836116.

436 24. Power DA, Watson RA, Szathmáry E, Mills R, Powers ST, Doncaster CP, et al. What can  
437 ecosystems learn? Expanding evolutionary ecology with learning theory. *Biol Direct.* 2015;10(1):69.  
438 doi:10.1186/s13062-015-0094-1.

439 25. Gonze D, Lahti L, Raes J, Faust K. Multi-stability and the origin of microbial community types.  
440 *ISME J.* 2017;11(10):2159. doi:10.1038/ismej.2017.60.

441 26. Gibson T, Gerber G. Robust and Scalable Models of Microbiome Dynamics. In: Proceedings of  
442 the 35th International Conference on Machine Learning. vol. 80. PMLR; 2018. p. 1763–1772.

443 27. Marino S, Baxter NT, Huffnagle GB, Petrosino JF, Schloss PD. Mathematical modeling of primary  
444 succession of murine intestinal microbiota. *Proc Natl Acad Sci USA.* 2014;111(1):439–444.

445 28. Stein RR, Bucci V, Toussaint NC, Buffie CG, Rätsch G, Pamer EG, et al. Ecological modeling from  
446 time-series inference: insight into dynamics and stability of intestinal microbiota. *PLoS Comput  
447 Biol.* 2013;9(12):e1003388. doi:10.1371/journal.pcbi.1003388.

448 29. Bucci V, Tzen B, Li N, Simmons M, Tanoue T, Bogart E, et al. MDSINE: Microbial Dynamical  
449 Systems INference Engine for microbiome time-series analyses. *Genome Biol.* 2016;17(1):1–17.  
450 doi:10.1186/s13059-016-0980-6.

451 30. Li C, Chng KR, Kwah JS, Av-Shalom TV, Tucker-Kellogg L, Nagarajan N. An  
452 expectation-maximization algorithm enables accurate ecological modeling using longitudinal  
453 microbiome sequencing data. *Microbiome.* 2019;7(1):1–14. doi:10.1186/s40168-019-0729-z.

454 31. Joseph TA, Shenhav L, Xavier JB, Halperin E, Pe'er I. Compositional Lotka-Volterra  
455 describes microbial dynamics in the simplex. *PLoS Comput Biol.* 2020;16(5):e1007917.  
456 doi:10.1371/journal.pcbi.1007917.

457 32. McGeachie MJ, Sordillo JE, Gibson T, Weinstock GM, Liu YY, Gold DR, et al. Longitudinal  
458 prediction of the infant gut microbiome with dynamic bayesian networks. *Sci Rep.* 2016;6:20359.  
459 doi:10.1038/srep20359.

460 33. Falony G, Joossens M, Vieira-Silva S, Wang J, Darzi Y, Faust K, et al. Population-level analysis of  
461 gut microbiome variation. *Science.* 2016;352(6285):560–564. doi:10.1126/science.aad3503.

462 34. Arumugam M, Raes J, Pelletier E, Le Paslier D, Yamada T, Mende DR, et al. Enterotypes of the  
463 human gut microbiome. *Nature.* 2011;473(7346):174–180. doi:10.1038/nature09944.

464 35. Ding T, Schloss PD. Dynamics and associations of microbial community types across the human  
465 body. *Nature.* 2014;509(7500):357–360. doi:10.1038/nature13178.

466 36. Costea PI, Hildebrand F, Arumugam M, Bäckhed F, Blaser MJ, Bushman FD, et al. Enterotypes  
467 in the landscape of gut microbial community composition. *Nat Microbiol.* 2018;3(1):8–16.  
468 doi:10.1038/s41564-017-0072-8.

469 37. Du M, Wang Z, Hu H. Measuring memory with the order of fractional derivative. *Sci Rep.*  
470 2013;3(1):1–3. doi:10.1038/srep03431.

471 38. Saeedian M, Khalighi M, Azimi-Tafreshi N, Jafari GR, Ausloos M. Memory effects on epidemic  
472 evolution: The susceptible-infected-recovered epidemic model. *Phys Rev E.* 2017;95:022409.  
473 doi:10.1103/PhysRevE.95.022409.

474 39. Venturelli OS, Carr AV, Fisher G, Hsu RH, Lau R, Bowen BP, et al. Deciphering microbial  
475 interactions in synthetic human gut microbiome communities. *Mol Syst Biol.* 2018;14(6):e8157.  
476 doi:<https://doi.org/10.15252/msb.20178157>.

477 40. Marrec L, Bitbol AF. Resist or perish: Fate of a microbial population subjected to a periodic presence  
478 of antimicrobial. *PLoS Comput Biol.* 2020;16(4):e1007798. doi:10.1371/journal.pcbi.1007798.

479 41. Rivero M, Rogosin SV, Tenreiro Machado JA, Trujillo JJ. Stability of fractional order systems.  
480 *Math Probl Eng.* 2013;2013:356215. doi:10.1155/2013/356215.

481 42. Spanbauer TL, Allen CR, Angeler DG, Eason T, Fritz SC, Garmestani AS, et al. Prolonged  
482 instability prior to a regime shift. *PLoS One.* 2014;9(10). doi:10.1371/journal.pone.0108936.

483 43. Tropini C, Moss EL, Merrill BD, Ng KM, Higginbottom SK, Casavant EP, et al. Transient osmotic  
484 perturbation causes long-term alteration to the gut microbiota. *Cell.* 2018;173(7):1742–1754.  
485 doi:10.1016/j.cell.2018.05.008.

486 44. Hastings A, Abbott KC, Cuddington K, Francis T, Gellner G, Lai YC, et al. Transient phenomena  
487 in ecology. *Science*. 2018;361(6406):eaat6412. doi:10.1126/science.aat6412.

488 45. Khalighi M, Eftekhari L, Hosseinpour S, Lahti L. Three-species Lotka-Volterra model  
489 with respect to Caputo and Caputo-Fabrizio fractional operators. *Symmetry*. 2021;13(3):368.  
490 doi:10.3390/sym13030368.

491 46. Shade A, Peter H, Allison S, Baho D, Berga M, Buergmann H, et al. Fundamentals of Microbial  
492 Community Resistance and Resilience. *Front in Microbiol*. 2012;3. doi:10.3389/fmicb.2012.00417.

493 47. Sommer F, Anderson JM, Bharti R, Raes J, Rosenstiel P. The resilience of the intestinal microbiota  
494 influences health and disease. *Nat Rev Microbiol*. 2017;15(10):630–638. doi:10.1038/nrmicro.2017.58.

495 48. Khazaei T, Williams RL, Bogatyrev SR, Doyle JC, Henry CS, Ismagilov RF. Metabolic multistability  
496 and hysteresis in a model aerobe-anaerobe microbiome community. *Sci Adv*. 2020;6(33):eaba0353.  
497 doi:10.1126/sciadv.aba0353.

498 49. Bush T, Diao M, Allen RJ, Sinnige R, Muyzer G, Huisman J. Oxic-anoxic regime shifts mediated  
499 by feedbacks between biogeochemical processes and microbial community dynamics. *Nat Commun*.  
500 2017;8(1):1–9. doi:<https://doi.org/10.1038/s41467-017-00912-x>.

501 50. Goyal A, Dubinkina V, Maslov S. Multiple stable states in microbial communities explained by  
502 the stable marriage problem. *ISME J*. 2018;12(12):2823–2834. doi:10.1038/s41396-018-0222-x.

503 51. Miller AD, Inamine H, Buckling A, Roxburgh SH, Shea K. How disturbance history alters invasion  
504 success: biotic legacies and regime change. *Ecol Lett*. 2021;24(4):687–697. doi:10.1111/ele.13685.

505 52. Yen P, Papin JA. History of antibiotic adaptation influences microbial evolutionary dynamics  
506 during subsequent treatment. *PLoS Biol*. 2017;15(8):1–34. doi:10.1371/journal.pbio.2001586.

507 53. Hutchinson GE. The paradox of the plankton. *Am Nat*. 1961;95(882):137–145. doi:10.1086/282171.

508 54. Huston M. A general hypothesis of species diversity. *Am Nat*. 1979;113(1):81–101.  
509 doi:10.1086/283366.

510 55. Abreu CI, Andersen Woltz VL, Friedman J, Gore J. Microbial communities display  
511 alternative stable states in a fluctuating environment. *PLoS Comput Biol*. 2020;16(5):1–17.  
512 doi:10.1371/journal.pcbi.1007934.

513 56. Knights D, Ward TL, McKinlay CE, Miller H, Gonzalez A, McDonald D,  
514 et al. Rethinking “Enterotypes”. *Cell Host & Microbe*. 2014;16(4):433–437.  
515 doi:<https://doi.org/10.1016/j.chom.2014.09.013>.

516 57. Sun H, Zhang Y, Baleanu D, Chen W, Chen Y. A new collection of real world applications of  
517 fractional calculus in science and engineering. *Commun Nonlinear Sci Numer Simul.* 2018;64:213–231.  
518 doi:10.1016/j.cnsns.2018.04.019.

519 58. Almeida R, Bastos NR, Monteiro MTT. Modeling some real phenomena by fractional differential  
520 equations. *Math Methods Appl Sci.* 2016;39(16):4846–4855. doi:10.1002/mma.3818.

521 59. Arani BMS, Carpenter SR, Lahti L, van Nes EH, Scheffer M. Exit time as a measure of ecological  
522 resilience. *Science.* 2021;372(6547). doi:10.1126/science.aay4895.

523 60. Achar BNN, Hanneken JW, Clarke T. Response characteristics of a fractional oscillator. *Physica  
524 A.* 2002;309(3):275–288. doi:10.1016/S0378-4371(02)00609-X.

525 61. Tarasov VE. Quantum dissipation from power-law memory. *Ann Phys (N Y).* 2012;327(6):1719–1729.  
526 doi:10.1016/j.aop.2012.02.011.

527 62. Morozov A, Abbott K, Cuddington K, Francis T, Gellner G, Hastings A, et al. Long transients in  
528 ecology: Theory and applications. *Phys Life Rev.* 2020;32:1–40. doi:10.1016/j.plrev.2019.09.004.

529 63. Fukami T. Assembly history interacts with ecosystem size to influence species diversity. *Ecology.*  
530 2004;85(12):3234–3242. doi:10.1890/04-0340.

531 64. Sun H, Chang A, Zhang Y, Chen W. A review on variable-order fractional differential equations:  
532 mathematical foundations, physical models, numerical methods and applications. *Fract Calc Appl  
533 Anal.* 2019;22(1):27–59. doi:10.1515/fca-2019-0003.

534 65. Cooke KL, Grossman Z. Discrete delay, distributed delay and stability switches. *J Math Anal  
535 Appl.* 1982;86(2):592–627. doi:10.1016/0022-247X(82)90243-8.

536 66. Zúñiga-Aguilar C, Coronel-Escamilla A, Gómez-Aguilar J, Alvarado-Martínez V, Romero-Ugalde  
537 H. New numerical approximation for solving fractional delay differential equations of variable order  
538 using artificial neural networks. *Eur Phys J Plus.* 2018;133(2):1–16. doi:10.1140/epjp/i2018-11917-0.

539 67. Wang JL, Li HF. Memory-dependent derivative versus fractional derivative (I): Difference in  
540 temporal modeling. *J Comput Appl Math.* 2021;384:112923. doi:10.1016/j.cam.2020.112923.

541 68. Tarasov VE. Rules for Fractional-Dynamic Generalizations: Difficulties of Constructing Fractional  
542 Dynamic Models. *Mathematics.* 2019;7(6). doi:10.3390/math7060554.

543 69. Diethelm K, Garrappa R, Giusti A, Stynes M. Why fractional derivatives with nonsingular kernels  
544 should not be used. *Fract Calc Appl Anal.* 2020;23(3):610–634. doi:doi:10.1515/fca-2020-0032.

545 70. Faust K, Lahti L, Gonze D, de Vos WM, Raes J. Metagenomics meets time series analysis: unraveling  
546 microbial community dynamics. *Curr Opin Microbiol.* 2015;25:56–66. doi:10.1016/j.mib.2015.04.004.

547 71. Armstrong McKay DI, Dyke JG, Doncaster CP, Dearing JA, Wang R. Network-based metrics of  
548 resilience and ecological memory in lake ecosystems. *bioRxiv.* 2020;doi:10.1101/810762.

549 72. Balakrishnan R, de Silva RT, Hwa T, Cremer J. Suboptimal resource allocation in changing  
550 environments constrains response and growth in bacteria. *Mol Syst Biol.* 2021;17:e10597.  
551 doi:10.15252/msb.202110597.

552 73. Gauffin Cano P, Santacruz A, Moya A, Sanz Y. *Bacteroides uniformis* CECT 7771 Ameliorates  
553 Metabolic and Immunological Dysfunction in Mice with High-Fat-Diet Induced Obesity. *PLoS*  
554 *ONE.* 2012;7(7):1–16. doi:10.1371/journal.pone.0041079.

555 74. Bloom S, Bijanki V, Nava G, Sun L, Malvin N, Donermeyer D, et al. Commensal *Bacteroides*  
556 Species Induce Colitis in Host-Genotype-Specific Fashion in a Mouse Model of Inflammatory Bowel  
557 Disease. *Cell Host Microbe.* 2011;9(5):390–403. doi:<https://doi.org/10.1016/j.chom.2011.04.009>.

558 75. Larsen N, Vogensen FK, van den Berg FWJ, Nielsen DS, Andreasen AS, Pedersen BK, et al. Gut  
559 Microbiota in Human Adults with Type 2 Diabetes Differs from Non-Diabetic Adults. *PLoS ONE.*  
560 2010;5(2):1–10. doi:10.1371/journal.pone.0009085.

561 76. Podlubny I. Fractional differential equations: An introduction to fractional derivatives, fractional  
562 differential equations, to methods of their solution and some of their applications. Elsevier; 1998.

563 77. Safdari H, Kamali MZ, Shirazi A, Khalighi M, Jafari G, Ausloos M. Fractional dynamics  
564 of network growth constrained by aging node interactions. *PLoS One.* 2016;11(5):e0154983.  
565 doi:10.1371/journal.pone.0154983.

566 78. Tarasova VV, Tarasov VE. Concept of dynamic memory in economics. *Commun Nonlinear Sci*  
567 *Numer Simul.* 2018;55:127–145. doi:<https://doi.org/10.1016/j.cnsns.2017.06.032>.

568 **Supporting information**

569 **S1 Appendix:** Methodological details for Fig 5c and S1 Fig

570 **S2 Appendix:** Numerical simulations

571 **S1 Table:** Exact model specifications for the 2, 3, and 15-species Gonze model (equation (1) in  
572 Methods)

573       **S2 Table:** Exact model specifications for the 2-species model given by equation (2) in Methods,  
574        and for the logistic growth curve in Fig 7

575       **S1 Fig:** Memory effects preserve the stable state in randomly structured communities

576       **S2 Fig:** Memory in a group of species decreases their relative abundance

577       **S3 Fig:** Impact of incommensurate memory in the presence of perturbation

578       **S4 Fig:** Memory can induce long transient dynamics even in the absence of multistability

579       **S5 Fig:** Memory effects on convergence time for different two-species community types

580       **S6 Fig:** Impact of memory on resistance to a pulse perturbation in the two-species version of  
581        Gonze multistable model

582       **S7 Fig:** Impact of memory on resistance to a pulse perturbation in a two-species community  
583        exhibiting bistability between dominance of *Bacteroides uniformis* (BU) and *Bacteroides thetaiotaomicron*  
584       (BT)

585       **S8 Fig:** Impact of memory on resilience after a pulse perturbation in the two-species version of  
586        Gonze multistable model

587       **S9 Fig:** Impact of memory on resilience after a pulse perturbation in a two-species community  
588        exhibiting bistability between dominance of *Bacteroides uniformis* (BU) and *Bacteroides thetaiotaomicron*  
589       (BT)

590       **S10 Fig:** Impact of memory on convergence time in the two-species version of Gonze multistable  
591        model

592       **S11 Fig:** Impact of memory on convergence time in a two-species community exhibiting bistability  
593        between dominance of *Bacteroides uniformis* (BU) and *Bacteroides thetaiotaomicron* (BT)

594       **S12 Fig:** Impact of memory on convergence time in a two-species community exhibiting stable  
595        coexistence between *Eubacterium rectale* (ER) and *Clostridium hiranonis* (CH)

596       **S13 Fig:** Impact of memory on convergence time in a two-species community exhibiting stable  
597        dominance of *Clostridium hiranonis* (CH) by *Bacteroides thetaiotaomicron* (BT)